

## Electronic Supplementary Information

3D hierarchical porous amidoxime fibers speed up uranium extraction from seawater

Xiao Xu<sup>1,3</sup>, Hongjun Zhang<sup>2</sup>, Junxuan Ao<sup>1,4</sup>, Lu Xu<sup>1</sup>, Xiyun Liu<sup>1</sup>, Xiaojing Guo<sup>5</sup>, Jingye Li<sup>1</sup>, Lan Zhang<sup>1</sup>, Qingnuan Li<sup>1</sup>, Xiaoyan Zhao<sup>3</sup>, Bangjiao Ye<sup>2</sup>, Deli Wang<sup>6</sup>, Fei Shen<sup>4,7</sup>,  
Hongjuan Ma<sup>1,\*</sup>

<sup>1</sup>Shanghai Institute of Applied Physics, Chinese Academy of Sciences, Shanghai 201800, China

<sup>2</sup>State Key Laboratory of Particle Detection and Electronics, University of Science and Technology of China, Hefei 230026, China

<sup>3</sup>School of Petrochemical Engineering, Changzhou University, Changzhou 213164, China

<sup>4</sup>University of Chinese Academy of Sciences, Beijing 100049, China

<sup>5</sup>The department of Chemistry and Chemical Engineering, Shanghai Normal University, Shanghai 200234, China

<sup>6</sup>State key Laboratory of Marine Environmental Science, Xiamen University, Xiamen 361005, China

<sup>7</sup>Institute of Process Engineering, Chinese Academy of Sciences, Beijing 100190, China

\*Corresponding author. *E-mail address:* [mahongjuan@sinap.ac.cn](mailto:mahongjuan@sinap.ac.cn)

## Table of Contents

1. Materials .....	3
2. Synthesis of H-ABP fiber.....	3
3. Synthesis of ABP fiber .....	6
4. Marine test in natural seawater.....	7
5. Adsorption capacity and service life of H-ABP fiber.....	8
6. Characterization techniques.....	10
7. Positron annihilation lifetime (PAL) spectroscopy .....	11
8. Supplementary Figures S1-S9 and Tables S1-S4.....	12

## 1. Materials

PE-coated PP skin-core fiber (PE/PP) was supplied by Haining Xin Gao Fibers Co., Ltd. 2-hydroxyethyl acrylate (HEA), copper(II) sulfate pentahydrate ( $\text{CuSO}_4 \cdot 5\text{H}_2\text{O}$ ), acrylonitrile (AN), acrylic acid (AA), ceric ammonium nitrate (CAN), nitric acid ( $\text{HNO}_3$ ), N,N-dimethylformamide (DMF), sodium carbonate ( $\text{Na}_2\text{CO}_3$ ), sodium bicarbonate ( $\text{NaHCO}_3$ ), sodium chloride (NaCl), sodium hydroxide (NaOH), hydrochloric acid (HCl), hydroxylamine hydrochloride ( $\text{NH}_2\text{OH} \cdot \text{HCl}$ ) and dimethyl sulfoxide (DMSO) were purchased from Sinopharm Chemical Reagent Company. All chemicals from commercial sources were of reagent grade and used without further purification. Nitrogen gas (99.99% purity) was obtained from Shanghai Louyang Gas Canned Co., Ltd. Baysalt was obtained from the salt fields in Qingdao, Shandong Province, China, and used without any refining. The 1,000 ppm standard solutions of uranium and competing ions were purchased from SPEX Certi Prep, Inc. High-purity deionized water (PALL, Cascada BIO) was used for all experiments unless otherwise stated.

## 2. Synthesis of H-ABP fibers

Commercial PE/PP fibers were used as substrate materials for the preparation of the H-ABP fiber. The H-ABP fiber was synthesized via pre-irradiation induced grafted polymerization of HEA, which provided the hydroxyl group (-OH). -OH could provide active sites for redox initiator  $\text{Ce}^{4+}$  to induce co-grafted polymerization of AN and AA. Then, the grafted fiber was amidoximated with  $\text{NH}_2\text{OH} \cdot \text{HCl}$  to obtain the amidoxime (AO,  $-\text{CNH}_2\text{N}-\text{OH}$ ) functional group.

The PE/PP fiber was pre-irradiated with  $^{60}\text{Co}$   $\gamma$ -rays in air at room temperature at a dose rate of 1.7 kGy/h. The absorbed dose ranged from 5 to 30 kGy. After irradiation, the pre-irradiated PE/PP fiber was placed in a flask containing monomer solution and then purged with nitrogen gas for 20 min to remove the oxygen. The monomer solution was composed of 20 vol% HEA, 80 vol%  $\text{H}_2\text{O}$ , and  $1 \times 10^{-3}$  mol/L  $\text{CuSO}_4 \cdot 5\text{H}_2\text{O}$ . Graft polymerization was performed in a water bath for 4 h at  $70^\circ\text{C}$ . Subsequently, the poly-HEA grafted fibers (PE/PP-*g*-PHEA) were washed with  $\text{H}_2\text{O}$  to remove homopolymer and residual monomers and dried with a vacuum oven at  $60^\circ\text{C}$ . The DG of grafted PHEA was calculated as follows:

$$DG(\%) = \frac{M_1 - M_0}{M_0} \times 100, \quad (1)$$

where  $M_0$  is the weight of the original PE/PP fiber and  $M_1$  is the weight of the PE/PP-*g*-PHEA fiber.

PE/PP-*g*-PHEA fiber with a DG of 10-20% can provide appropriate -OH activation sites for subsequent CIGP of AN and AA. Accordingly, the effect of absorbed dose in the range of 0-30 kGy on the DG of the PE/PP-*g*-PHEA fibers was investigated. As shown in Supplementary Fig. 1a, the DG of HEA increased linearly with increasing absorbed dose and reached 15% at 10 kGy (with 20 vol% monomer concentration, and at  $70^\circ\text{C}$  after grafting for 4 h). A higher absorbed dose of 30 kGy resulted with a higher DG of 54.2%. However, taking into account the radiation damage of the trunk PE/PP fiber and energy consumption, the relatively lower absorbed dose of 10 kGy, a reaction time of 4 h, a reaction temperature of  $70^\circ\text{C}$  and a monomer concentration of 20 vol%

were identified as the optimum conditions and exploited for the preparation of PE/PP-*g*-PHEA fibers whose DG was 15% under such conditions.

Subsequently, PE/PP-*g*-PHEA fibers with a DG of 0-54.2% were immersed in a flask containing a monomer solution of AA/AN/DMF (12 vol%/48 vol%/40 vol%). After purging with nitrogen gas for 10 min, 5 mL of stock Ce<sup>4+</sup> solution (0.1 mol/L CAN in 1 mol/L HNO<sub>3</sub>) were added to the monomer solution immediately. The co-grafting polymerization was performed in a water bath for 0-10 h at 35-85°C. After grafting, the poly-AA and poly-AN co-grafting (PE/PP-*g*-PHEA-(PAA-*co*-PAN)) fibers were washed with DMF to remove residual monomers and homopolymers and dried in a vacuum oven at 60°C. The DG of the PE/PP-*g*-PHEA-(PAA-*co*-PAN) fibers was calculated as follows:

$$DG(\%) = \frac{M_2 - M_1}{M_1} \times 100, \quad (2)$$

where  $M_1$  is the weight of the PE/PP-*g*-PHEA fiber and  $M_2$  is the weight of the PE/PP-*g*-PHEA-(PAA-*co*-PAN) fiber.

The effects of PE/PP-*g*-PHEA fiber DG, reaction time and reaction temperature on the DG of PE/PP-*g*-PHEA-(PAA-*co*-PAN) fibers were investigated. As shown in Supplementary Fig. 1b-d, the results showed that the DG of PE/PP-*g*-PHEA-(PAA-*co*-PAN) increased with the increasing DG of PE/PP-*g*-PHEA fibers in the range of 0-54.2%. At a DG of 15% for the PE/PP-*g*-PHEA fibers, the DG of PE/PP-*g*-PHEA-(PAA-*co*-PAN) increased with an increase in the reaction time and a saturation of 138.4% was reached after 8 h. Temperature is an important factor for the CIGP of AN and AA as high temperatures promote homopolymer formation. Adsorption

applications require a DG of 100-150% with an appropriate density and utilization percentage of functional groups. Accordingly, the relatively lower DG of 15.0% for PHEA, a reaction time of 5 h and a reaction temperature of 45°C were identified as optimum conditions and were exploited for the preparation of PE/PP-g-PHEA-(PAA-co-PAN) fibers whose DG was 110.0% under such conditions.

Finally, 5 wt% solution of  $\text{NH}_2\text{OH}\cdot\text{HCl}$  was prepared using a bicomponent solvent composed of  $\text{H}_2\text{O}$  (50 vol%) and DMSO (50 vol%). The pH of the solution was adjusted to neutral with  $\text{Na}_2\text{CO}_3$ . The PE/PP-g-PHEA-(PAA-co-PAN) fibers were put into the 5 wt% solution of  $\text{NH}_2\text{OH}\cdot\text{HCl}$  at 25-85°C for 4 h to convert the nitrile groups into AO groups. After amidoximation, the H-ABP fibers were washed with deionized water to remove the unreacted  $\text{NH}_2\text{OH}$ , and then dried in a vacuum oven at 60°C. The AO group density of the H-ABP fibers was determined using the following equation:

$$AO \text{ Density (mmol/g)} = \frac{1000 \times (M_3 - M_2)}{33M_3} \times 100, \quad (3)$$

where  $M_2$  and  $M_3$  are the weights of PE/PP-g-PHEA-(PAA-co-PAN) and H-ABP fibers, respectively and 33 is the molecular weight of the AO group minus the molecular weight of the nitrile group.

### 3. Synthesis of ABP fibers

PE/PP fibers were pre-irradiated with  $^{60}\text{Co}$   $\gamma$ -rays in air at room temperature and a dose rate of 1.7 kGy/h. The absorbed dose was 80 kGy. After irradiation the pre-irradiated PE/PP fiber samples were placed in flasks containing monomer solution and then purged with nitrogen gas for 20 min to remove the oxygen. The monomer solution was

composed of 12 vol% AA, 48 vol% AN, and 40 vol% DMF. Graft polymerization was performed in a water bath for 5 h at 50°C. Subsequently, the grafted fibers were washed with DMF to remove homopolymers and residual monomers and were dried in a vacuum oven at 60°C. The 110.0% DG of the grafted fibers was calculated using Eq. (1). Subsequently, the amoximation was the same as that described above for H-ABP fibers. The AO group density of the ABP fiber was 6.8 mmol/g.

#### **4. Marine test in natural seawater**

The marine adsorption test was performed in the coastal area of Raoping, Guangdong Province, China (117.08° E, 23.58° N). A flow-through flume test platform was developed and used for the marine test in natural seawater (a record of the natural seawater adsorption equipment used is provided in the Supplementary Video). Salinity, pH and temperature of the natural seawater were obtained using handheld probes several times a week during the adsorption periods. The adsorption test in this study was carried out at an average pH of  $8.0\pm 0.1$ , salinity of  $29.6\pm 0.4$  psu, temperature of  $26.3\pm 0.5$ °C. The natural seawater was pumped to an underground impounded reservoir. After filtering out the sediment with a polyester non-woven fabric, the seawater was pumped into a flume (Fig. S9a and b, ESI†). The flow rate of the flume could be controlled with a motor controller. The inlet flow rate was adjusted to 1.5 L/min, the flume size was 152.6×8×15 cm and the flow velocity was 0.2 cm/s. H-ABP and ABP fibers were immersed in the flume. The duration of the marine test was 90 days. Three independent samples were collected for analysis. The collected samples were rinsed with deionized water three times and then dried in a vacuum oven at 60°C for 24 h. The

amount of extracted U, V, Fe, Co, Ni, Cu, Zn, Pb, Ca and Mg from H-ABP fibers and ABP fibers were analyzed by inductively coupled plasma atomic emission spectroscopy (ICP-AES) after digestion with microwave in nitric acid. The H-ABP fibers and ABP fibers were digested in 10 mL of high-purity concentrated nitric acid at a programmed temperature (25 min heating from 25 to 190°C, hold for 25 min followed by natural cooling) using a MARS6 Microwave Digestion System (CEM, USA). High-purity deionized water was then added to produce a 50 mL dilute acid solution and obtain a desired uranium concentration range for the analysis. The amount of uranium and other competing ions that were absorbed was calculated using the following equation:

$$Q = CV_d / M , \quad (4)$$

where  $Q$  (mg/g) is the adsorption capacity of the fiber for metal ions,  $C$  (mg/L) is the concentration of the measured metal ion by ICP-AES,  $V_d$  (L) is the digested solution volume and  $M$  (g) is the weight of the dried fiber after adsorption.

Concentration of uranium in natural seawater was determined using ICP-MS and the method of standard addition calibrations. Instrumental calibration curves were prepared in 20-fold diluted natural seawater spiked at four different concentration levels of 0.1, 0.2, 0.3, and 0.4 ppb with a 2% nitric acid blank. The natural seawater samples were then analyzed at 20-fold dilution with high-purity deionized water and then quantified using the matrix matched additions calibration curve. The standard nearshore seawater reference material (CASS-5) which was purchased from the National Research Council Canada was also analyzed at a 20-fold dilution every 10 samples to verify the analytical results. Concentration of competing ions V, Fe, Co, Ni, Cu, Zn and Pb in natural

seawater was determined using ICP-MS and the method of preconcentration techniques with Chelex-100 resin. Concentration of Ca and Mg was determined with ICP-AES after 500-fold dilution. Average concentration of uranium and competing ions in natural seawater were shown in Table S3 (ESI†).

## **5. Adsorption capacity and service life of H-ABP fibers**

Batch adsorption and 10 consecutive adsorption–desorption cycles were performed to study the adsorption capacity and reusability of the H-ABP fibers in simulated seawater system A and system B. Simulated seawater solution system A consisted of 193 ppm  $\text{NaHCO}_3$ , 25,600 ppm  $\text{NaCl}$ , and 8 ppm uranium, which was diluted with deionized water from its 1,000 ppm standard solution. The pH of system A was  $8.0 \pm 0.1$ . The concentrations of sodium and bicarbonate were selected to be similar to those of seawater. 0.02 g of H-ABP fiber was put into 1 L of system A solution for 24 h at room temperature with constant shaking at 100 rpm. After adsorption, 50 mL of 0.5 M HCl solution (at room temperature for 10 minutes) was used as the eluent and 20 mL of 5 mM NaOH solution (at room temperature for 5 minutes) was used for the regeneration. Following regeneration, the H-ABP fiber was rinsed with deionized water three times, and then used for the next uranium adsorption-desorption cycle following the same procedure as described above. The uranium content of the eluted solution was determined by inductively coupled plasma mass spectrometry (ICP-MS) with appropriate dilution. The uranium adsorption capacity of the H-ABP fibers can be determined from the following equation:

$$Q = CV / M , \quad (5)$$

where  $Q$  (mg/g) is the uranium adsorption capacity of the H-ABP fiber,  $C$  (mg/L) is the metal ion concentration measured by ICP-MS or ICP-AES,  $V$  (L) is the eluted solution volume and  $M$  (g) is the weight of the dried H-ABP fiber that was used.

Considering the low uranium concentration at the ppb level and the presence of competing ions in natural seawater, the simulated seawater system B was used to further confirm the adsorption capacity and service life of the H-ABP fiber. 175 g sea salt, certain amount of uranium and competing ions standard solutions were added in 5 L deionized water. The initial concentrations of uranium and competing metal ions  $\text{VO}^{3-}$ ,  $\text{Fe}^{3+}$ ,  $\text{Co}^{2+}$ ,  $\text{Ni}^{2+}$ ,  $\text{Cu}^{2+}$ ,  $\text{Zn}^{2+}$  and  $\text{Pb}^{2+}$  in the simulated seawater system were about 100 times higher than in natural seawater (Table S3, ESI†). The pH value was adjusted to  $8.0 \pm 0.1$  with  $\text{Na}_2\text{CO}_3$ . Next, 0.1 g of H-ABP fiber was put into 5 L plastic tanks of simulated seawater, which were prepared by dissolving a certain weight of sea salt into deionized water to produce a salinity of 35 practical salinity units (psu). The adsorption experiment was carried out on a rotary shaker at  $25^\circ\text{C}$  and 100 rpm for 24 h. The uranium and other metal ions loaded onto the H-ABP fibers were eluted into 50 mL of 0.5 M HCl solution at room temperature with a rotary shaker at 100 rpm for 1 h. The concentration of the eluted uranium was analyzed by ICP-AES with appropriate dilution. The adsorption capacity of the H-ABP fiber adsorbent for the various metal ions could be determined using Eq. (5). After elution, the H-ABP fibers were immersed in 20 mL of 5 mM NaOH solution at room temperature for 15 min was used for the regeneration, rinsed with deionized water three times, and then used for the next adsorption-desorption cycle following the same procedure as that described above.

## **6. Characterization techniques**

FT-IR spectra were collected in the attenuated total reflectance mode (Thermo Nicolet Company, USA). The elemental composition and chemical states of the fibers were analyzed by X-ray photoelectron spectroscopy (XPS) using a Thermo SCIENTIFIC ESCALAB 250Xi instrument. The XPS data were acquired through wide scans ranging from 0 to 1300 eV. The surface morphology of the fibers was viewed with a field-emission scanning electron microscope (SEM, JSM-6700F, JEOL, Japan) after sputtering with gold. Details regarding the loosened ellipsoidal polymer particle structure as well as swelling on the H-ABP fiber surfaces were further investigated using high-resolution environmental scanning electron microscopy (ESEM, FEI Quanta250, USA). To avoid a heating effect and damage to the surface chemistry caused by electron beam irradiation, the ESEM images were obtained under an electron beam potential of 20 kV, a spot size of 3.0 and a diaphragm diameter of 30  $\mu\text{m}$ . An atomic force microscope (AFM) instrument (NanoScope VIII, Bruker) equipped with a 100- $\mu\text{m}$  scanner and a liquid cell was used for the morphology and roughness measurements of the samples. The samples were fixed onto the iron sheet with double-sided tape, PE/PP and H-ABP fibers were subjected to air imaging after being blow dried, and H-ABP fibers were also immersed in high-purity deionized water for 3 days, which were used directly for AFM liquid imaging. Experiments were performed in Peak Force Quantitative NanoMechanical (PF-QNM) AFM mode. All AFM operations were carried out in air or liquid at room temperature. The NSC11 (MikroMash company) with a nominal spring constant of 40 N/m probe was used for imaging in the air, and

the DNP-S10 (Bruker company) with a nominal spring constant of 0.35 N/m probe was used for imaging in the liquid. Analysis of all the images was carried out using the Nanoscope software (Version 1.40). All images were shown without any image processing except for flattening. The BET surface area was acquired through nitrogen absorption-desorption on a surface aperture adsorption instrument (ASAP2010C, Micromeritics, USA). The fibers were embedded in epoxy resin and ultramicrotomed at -120°C to a section with a thickness of about 70 nm where the phase structure of the fiber cross section was observed directly using a transmission electron microscope (TEM, Jeol 2010) at an accelerated voltage of 200 kV. The Tensile strength of the fiber was tested on a universal testing machine (TIDJ-1000, Suzhou Zhuo Xu Precision Industry Co. Ltd., China). The concentrations of the metal ions in the simulated and real seawater were determined by ICP-AES (PerkinElmer Optima 8000). The average of two replicate measurements per sample was used to quantify uranium and other coexisting ions against a four-point calibration curve. ICP-MS (Perkin Elmer, NexION 300D) was used for quantitative analysis. The <sup>13</sup>C CP/MAS solid-state nuclear magnetic resonance (NMR) spectra were acquired on a Varian Inova 400 WB spectrometer.

## **7. Positron annihilation lifetime (PAL) spectroscopy**

PAL spectra were collected using a digital PAL spectrometer (DPLSAIO3000, Anhui Nuclear and Technology Ltd.) with a time resolution of ~179 ps. The positron source (<sup>22</sup>NaCl, ~3 μCi, fixed between two polyimide foils in the size of 10 mm×10 mm×7.5 μm) was sandwiched between two identical pellet samples (compressed under

a static pressure of 20 MPa) with a dimension of  $\Phi$  10 mm  $\times$  1 mm. Each PAL spectrum was collected for 4,096 channels with a channel width of 20 ps/channel. The total count of each PAL spectrum was  $1 \times 10^6$ , with a counting rate of around 85 cps.

In polymers, prior to the eventual annihilation, a positron could capture an electron to form a bound state, the so-called positronium (Ps) atom. A Ps atom could exist in one of two spin states: spin-singlet para-positronium and spin-triplet ortho-positronium (*o*-Ps). The *o*-Ps atoms collide with the walls of free-volume holes prior to their eventual annihilation. During the collisions, the positron of *o*-Ps picks up an electron with an opposite spin direction and annihilates into two  $\gamma$ -rays, which is usually called *o*-Ps pick-off annihilation. In polymers, the *o*-Ps pick-off annihilation is usually in the lifetime (time interval between the emitting of a positron and its eventual annihilation) range from 1 to 10 ns.

## 8. Supplementary Figures S1-S9 and Tables S1-S4



**Figure S1.** The mechanism for CIGP of AN and AA.

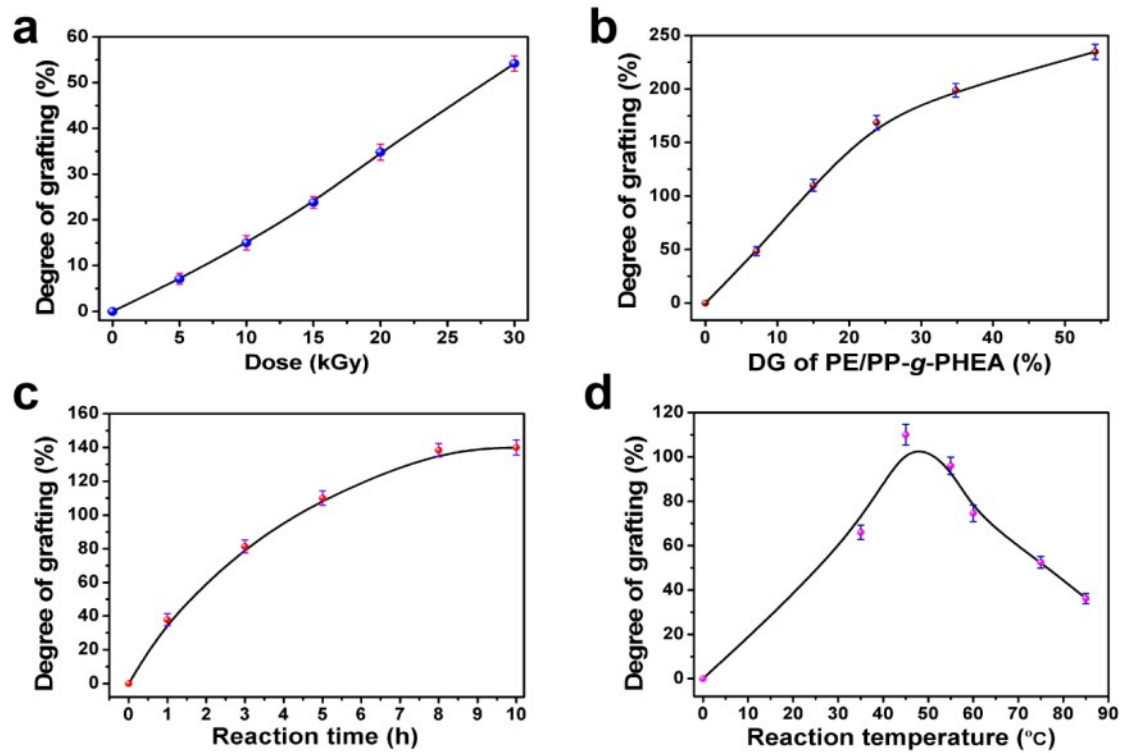


**Figure S2.** (a) DG of the PE/PP-g-PHEA fiber as a function of absorbed dose, (b) DG of the PE/PP-g-PHEA-(PAA-co-PAN) fiber as a function of DG of the PE/PP-g-PHEA fiber, (c) reaction time, (d) reaction temperature.

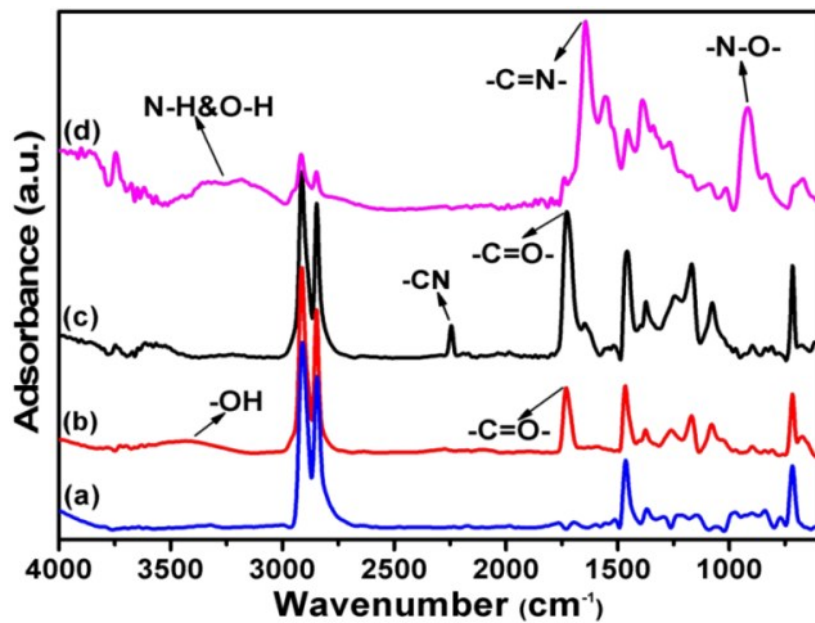


**Figure S3.** FT-IR spectra of (a) PE/PP, (b) PE/PP-g-PHEA, (c) PE/PP-g-PHEA-(PAA-co-PAN), and (d) H-ABP fiber.

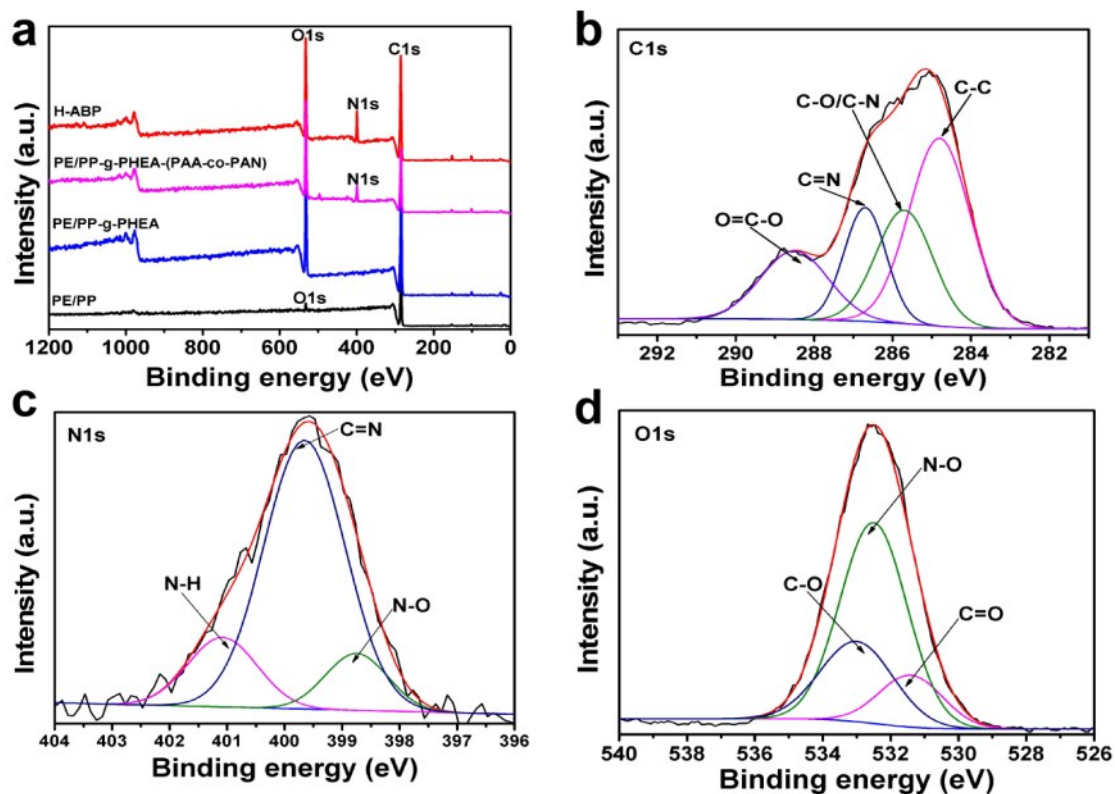


**Figure S4.** (a) XPS spectra of PE/PP, PE/PP-g-PHEA, PE/PP-g-PHEA-(PAA-co-PAN), and H-ABP fibers. The C 1s, N 1s, and O 1s (b, c, and d, respectively) spectra of the H-ABP fiber.

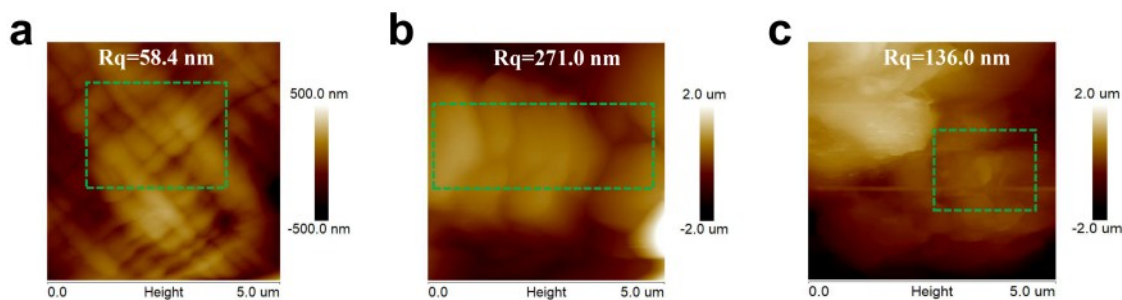


**Figure S5.** AFM images of (a) PE/PP and (b) H-ABP fibers, respectively. (c) AFM image of the H-ABP fiber in a wet state after soaking in deionized water for three days.

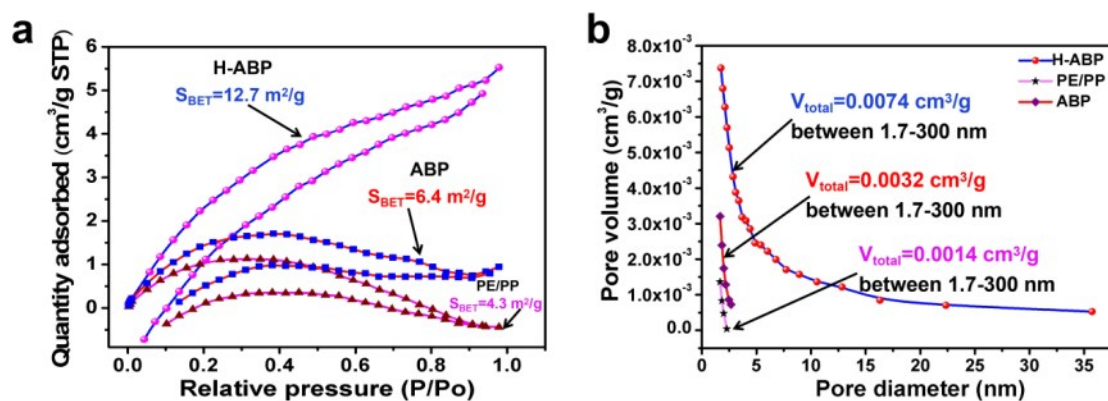


**Figure S6.** (a) N<sub>2</sub> sorption isotherms of the H-ABP, ABP and PE/PP fibers. (b) Pore diameter distributions of the H-ABP, ABP and PE/PP fibers.

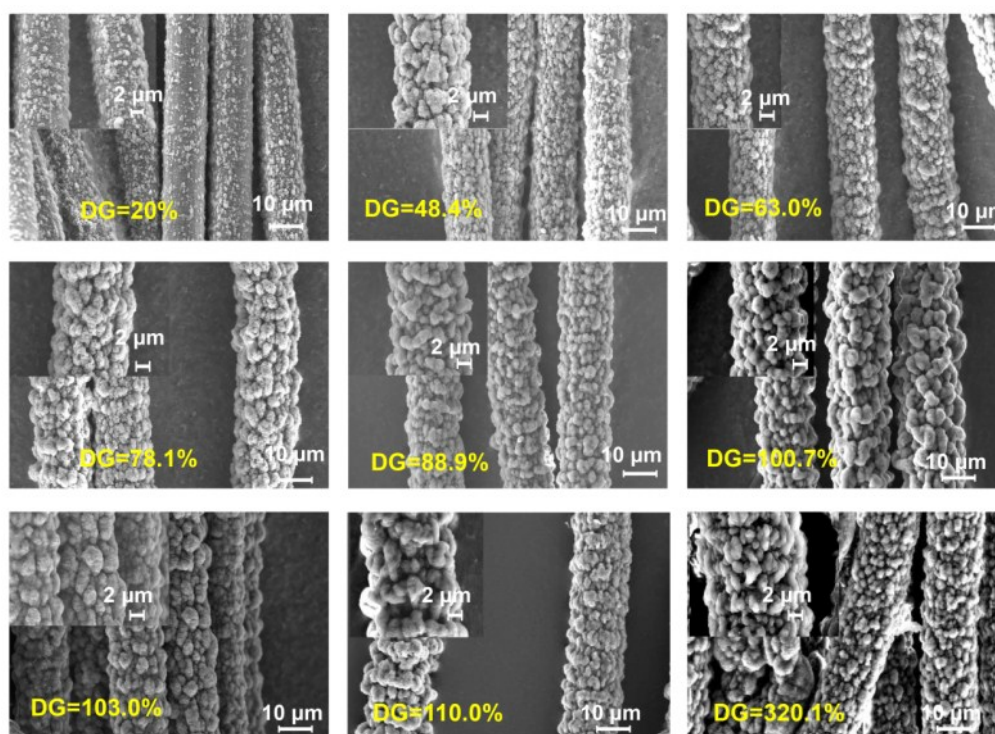


**Figure S7.** SEM images of the different DG of the PE/PP-g-PHEA-(PAA-co-PAN) fiber. The inset shows the structure of the different DG of the PE/PP-g-PHEA-(PAA-co-PAN) fiber at a higher magnification.

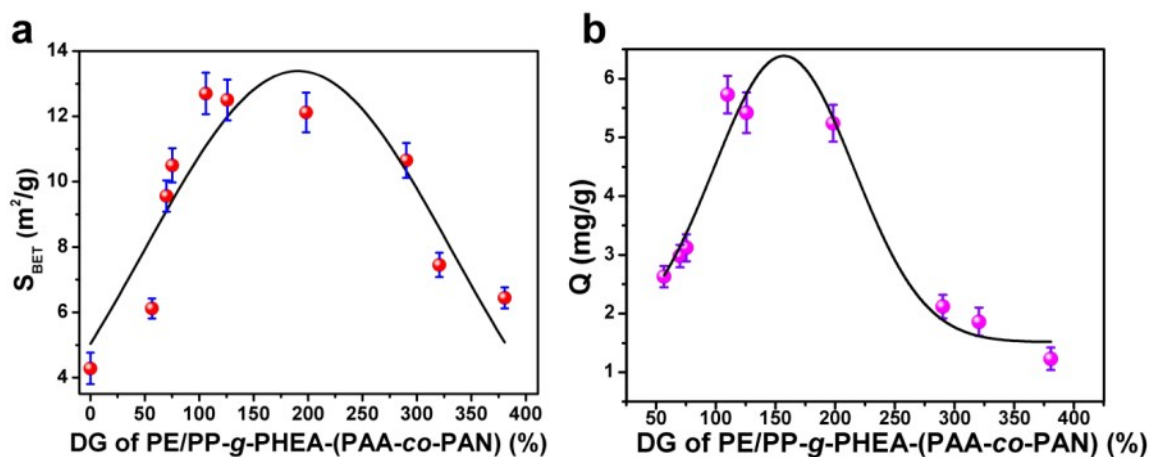


**Figure S8.** (a) BET surface area of H-ABP fiber as a function of DG of PE/PP-g-PHEA-(PAA-co-PAN) fiber. (b) Uranium-adsorption capacity of H-ABP fiber as a function of DG of PE/PP-g-PHEA-(PAA-co-PAN) fiber in simulated seawater.

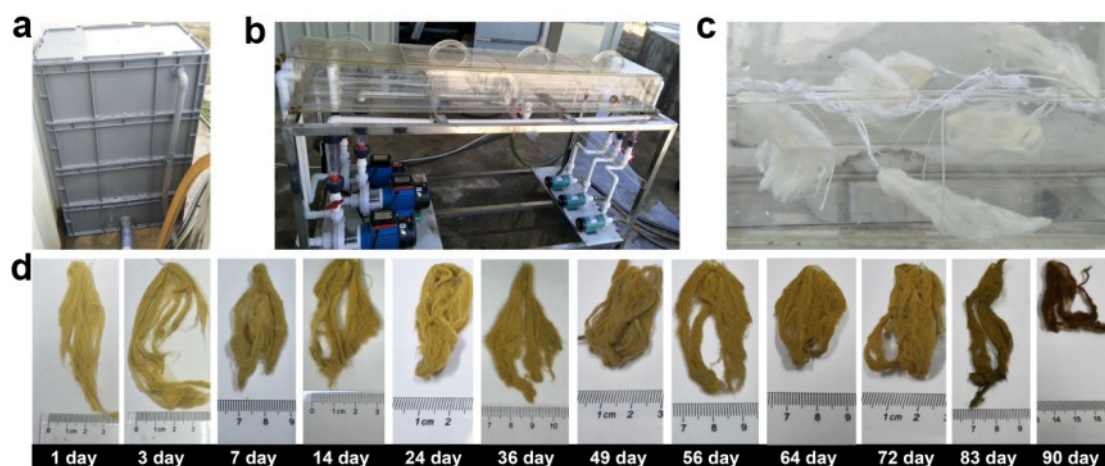


**Figure S9.** Recovery of uranium from natural seawater. (a) Seawater reservoir. (b) Adsorption flume. (c) H-ABP fibrous adsorbent immersed in the flume at the beginning of adsorption. (d) Photos of H-ABP fibrous adsorbent after adsorption in natural seawater at different time.

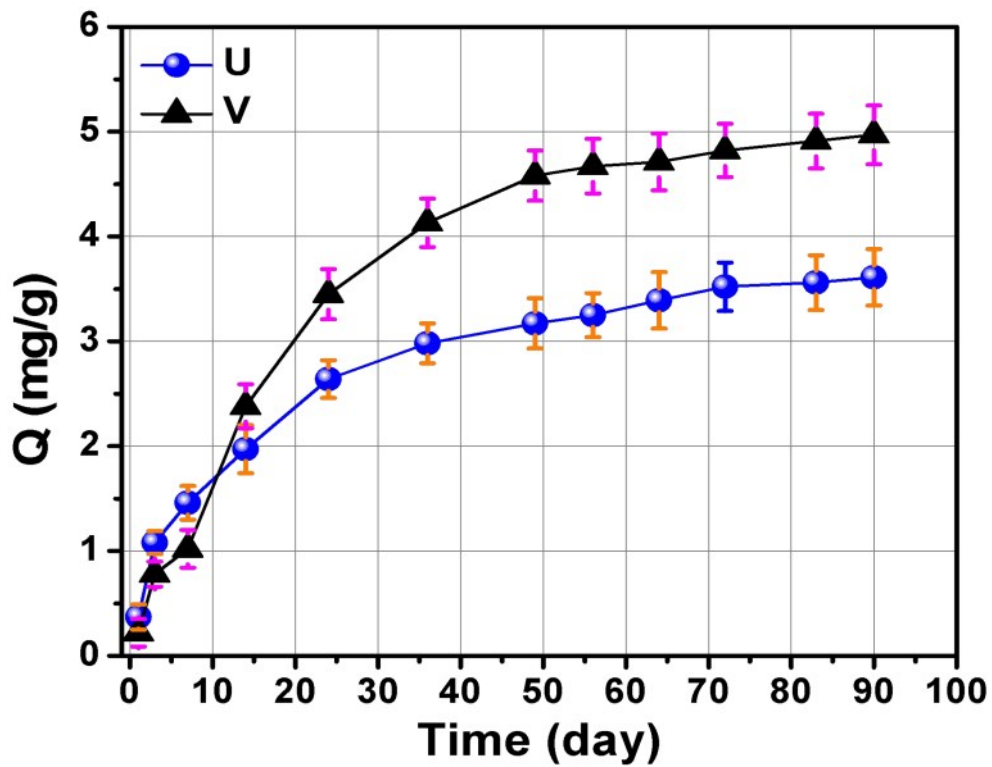


**Figure S10.** Adsorption capacity of U and V for ABP fiber during different periods with natural seawater during the marine test.

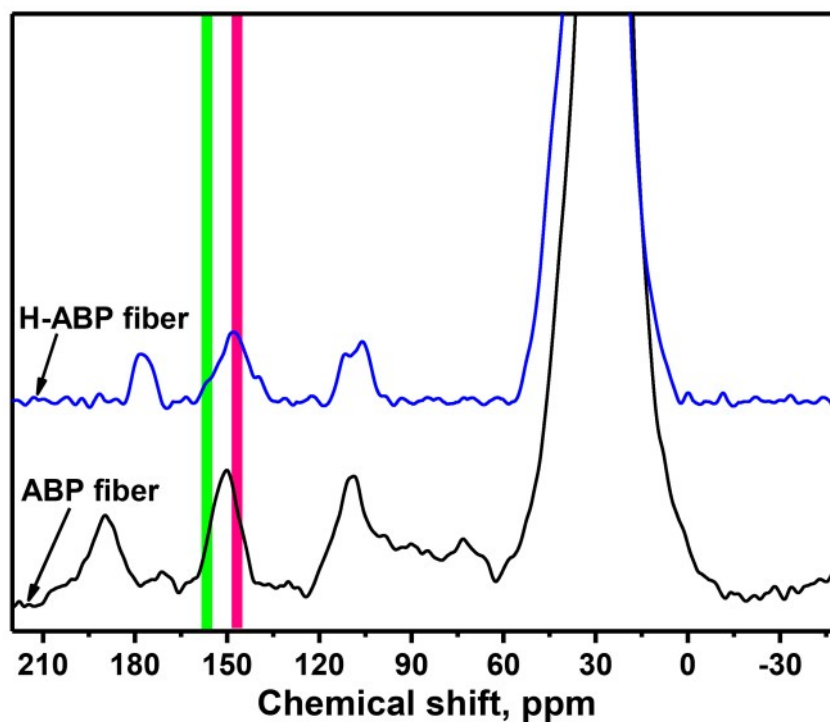


**Figure S11.**  $^{13}\text{C}$  CP/MAS spectra of H-ABP and ABP fibers.

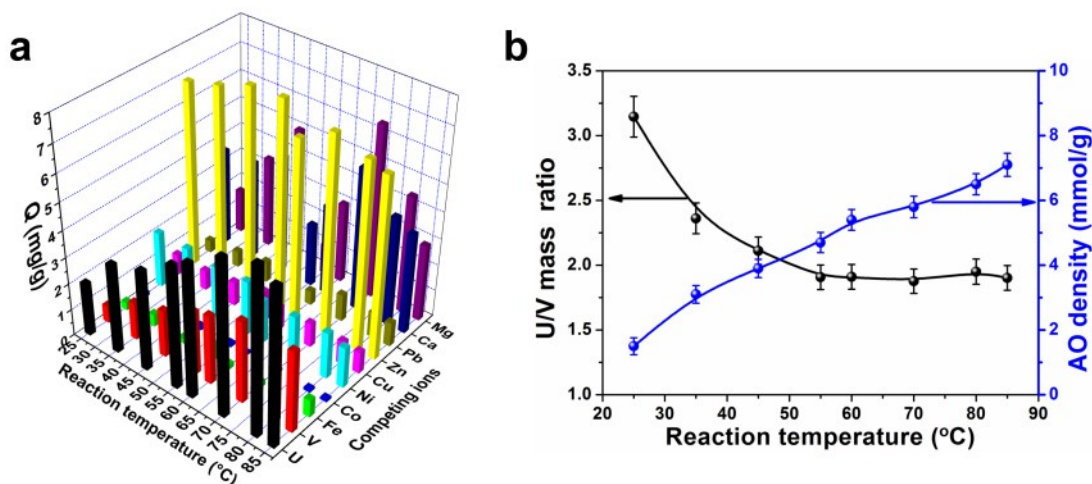


**Figure S12.** (a) Uranium adsorption capacity during the different reaction temperature of amidoximation of H-ABP fibers in simulated seawater system B with an initial uranium concentration of 330 ppb and coexisting ions of V, Fe, Ni, Cu, Zn, Pb, Co, Mg, and Ca. (b) U/V mass ratio (Left-Y-axis, black line) and AO density (Right-Y-axis, blue line) of the H-ABP fibers as a function of different reaction temperature of amidoximation.

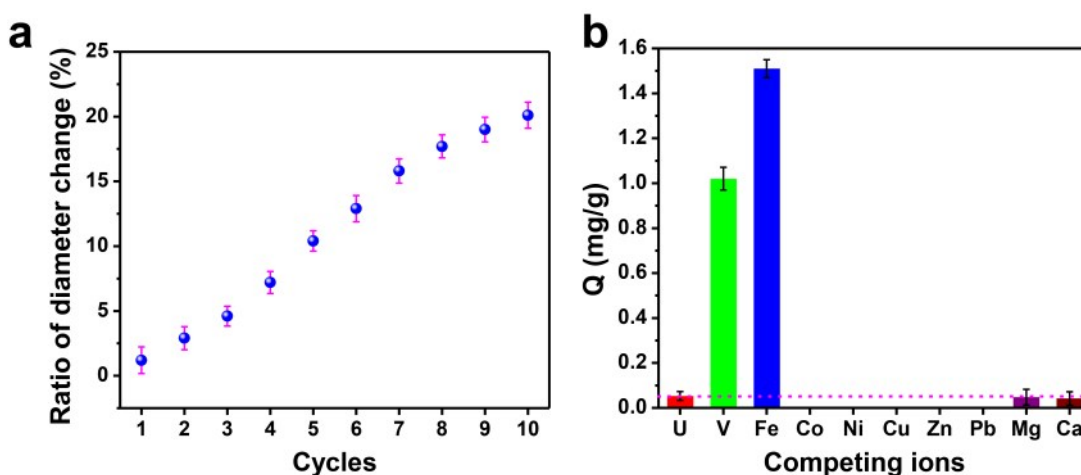


**Figure S13.** (a) Ratio of diameter change of H-ABP fibers during the 10 adsorption–desorption cycles in simulated seawater system B. (b) The residual amount of U and competing ions in H-ABP fibers after 10 adsorption–desorption cycles after digestion with microwave.

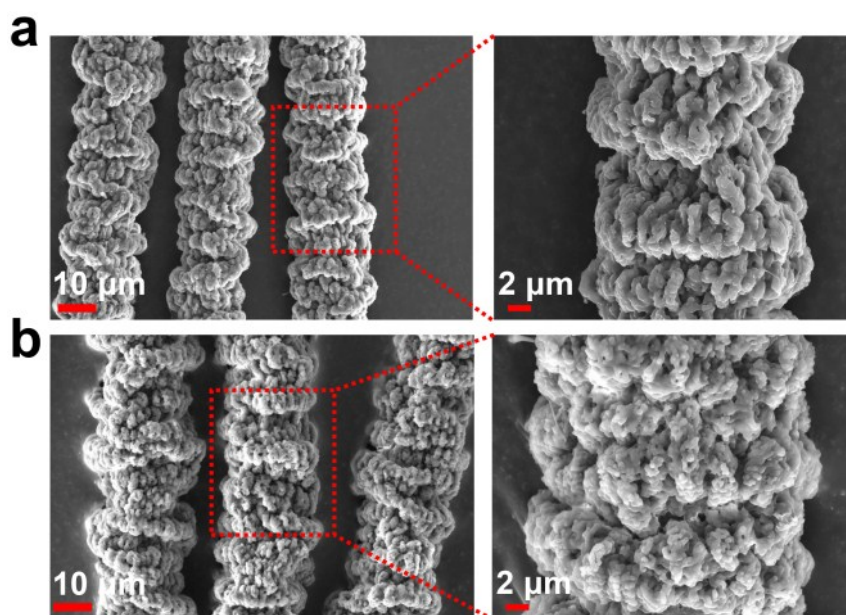


**Figure S14.** (a) SEM images of H-ABP fiber at different magnifications. (b) SEM images of H-ABP fiber after 10 adsorption–desorption cycles in simulated seawater system B at different magnifications.

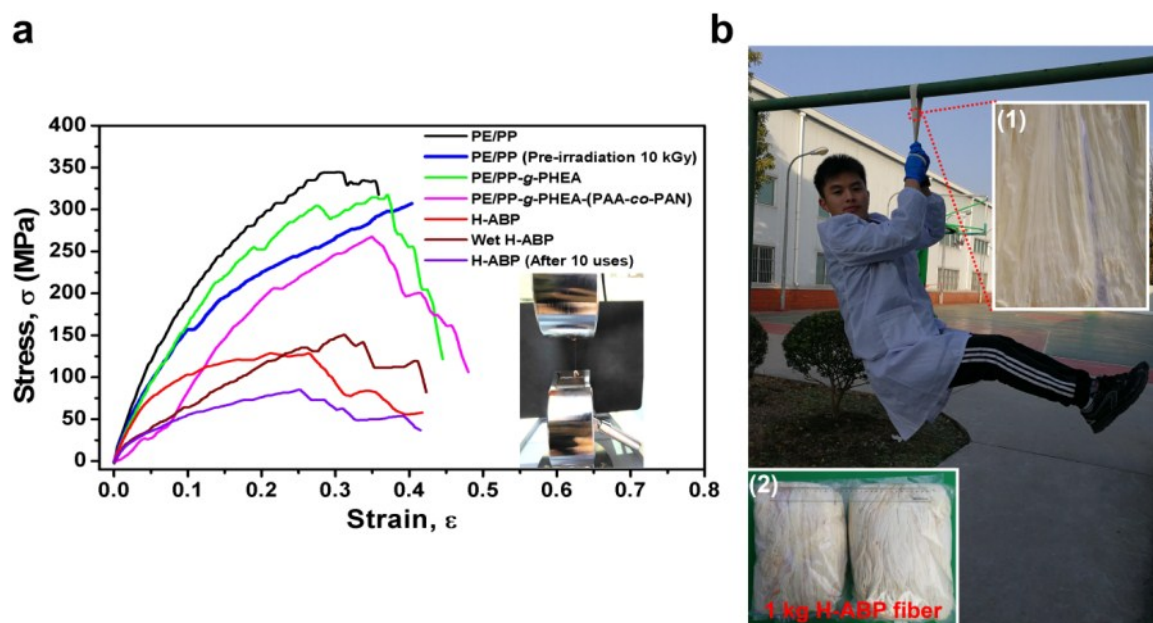


**Figure S15.** (a) The stress-strain curves of single PE/PP fiber, PE/PP fiber pre-irradiated with 10 kGy, PE/PP-g-PHEA fiber, PE/PP-g-PHEA-(PAA-co-PAN) fiber, H-ABP fiber, H-ABP fiber in a wet state and H-ABP fiber after 10 adsorption–desorption cycles in simulated seawater, respectively. The inset shows the photo of H-

ABP fibers mounted on universal testing machine. (b) The mechanical test shows that the H-ABP (5 g, 1 m) can hold a 60 kg weight of an adult steadily. Inset: (1) loose state of H-ABP fibers, which can be settled in seawater as seaweed; in particular, they are easy to be fabricate into various shapes and lengths. (2) Photograph of 1 kg H-ABP fiber.

**Table S1.** Average adsorption capacities (mg/g) of U, V, Fe, Co, Ni, Cu, Zn, Pb, Ca, and Mg for H-ABP fibers during different contact periods with natural seawater during the marine test.

<b>Time (day)</b>	<b>U</b>	<b>V</b>	<b>Fe</b>	<b>Co</b>	<b>Ni</b>	<b>Cu</b>	<b>Zn</b>	<b>Pb</b>	<b>Ca</b>	<b>Mg</b>
1	0.60	0.73	1.29	0.00	0.06	0.08	0.19	0.02	10.85	9.88
3	1.20	1.14	1.68	0.00	0.12	0.11	0.35	0.03	14.86	10.75
7	1.60	1.18	1.92	0.00	0.09	0.08	0.22	0.02	14.91	12.35
14	2.20	2.38	1.60	0.00	0.16	0.14	0.30	0.04	15.34	12.58
24	3.70	3.45	1.30	0.00	0.19	0.2	0.28	0.04	15.67	12.75
36	5.40	4.03	1.31	0.00	0.19	0.26	0.22	0.03	16.45	12.87
49	7.10	4.96	1.21	0.00	0.28	0.35	0.32	0.04	17.00	12.36
56	8.30	5.48	2.10	0.00	0.29	0.41	0.32	0.04	17.35	12.94
64	9.40	6.30	2.85	0.00	0.31	0.46	0.35	0.03	17.98	13.21
72	10.20	6.98	3.16	0.00	0.30	0.43	0.39	0.05	18.35	13.56
83	11.10	7.56	3.42	0.00	0.28	0.45	0.41	0.06	18.69	14.32
90	11.50	8.12	3.86	0.00	0.32	0.47	0.43	0.05	19.21	14.52

**Table S2.** Average adsorption capacities (mg/g) of U, V, Fe, Co, Ni, Cu, Zn, Pb, Ca, and Mg for ABP fiber during different contact periods with natural seawater during the marine test.

<b>Time (day)</b>	<b>U</b>	<b>V</b>	<b>Fe</b>	<b>Co</b>	<b>Ni</b>	<b>Cu</b>	<b>Zn</b>	<b>Pb</b>	<b>Ca</b>	<b>Mg</b>
1	0.37	0.22	0.11	0.00	0.02	0.06	0.06	0.01	5.16	8.36
3	1.08	0.78	0.62	0.00	0.05	0.10	0.13	0.01	6.22	7.74
7	1.46	1.02	0.23	0.00	0.07	0.11	0.19	0.02	8.87	8.62
14	1.97	2.38	0.73	0.00	0.16	0.14	0.30	0.04	11.48	11.81
24	2.64	3.45	0.90	0.00	0.19	0.20	0.28	0.04	12.17	12.66
36	2.98	4.13	0.91	0.00	0.16	0.13	0.24	0.03	12.67	11.29
49	3.17	4.58	0.58	0.00	0.25	0.20	0.24	0.04	13.06	11.67
56	3.25	4.67	0.79	0.00	0.28	0.24	0.27	0.05	13.24	12.67
64	3.39	4.71	1.66	0.00	0.18	0.13	0.25	0.03	14.67	14.42
72	3.52	4.82	1.37	0.00	0.14	0.19	0.22	0.02	14.78	14.24
83	3.56	4.91	1.28	0.00	0.26	0.23	0.26	0.04	15.24	14.35
90	3.61	4.97	1.31	0.00	0.27	0.27	0.25	0.06	15.63	14.62

**Table S3.** Ions concentration in natural seawater and simulated seawater (system B)

<b>Element</b>	<b>U</b>	<b>V</b>	<b>Fe</b>	<b>Co</b>	<b>Ni</b>	<b>Cu</b>	<b>Zn</b>	<b>Pb</b>	<b>Mg</b>	<b>Ca</b>
<b>Natural Seawater Conc. in this study (ppb)</b>	3.1	2.0	57.6	0.06	1.1	1.3	4.1	0.73	$1.2 \cdot 10^6$	$0.4 \cdot 10^6$
<b>Simulated Seawater Conc. in system B (ppb)</b>	330	152	141	5.3	101	65	408	34.6	$1.2 \cdot 10^5$	$0.6 \cdot 10^5$

**Table S4.** Adsorption capacity (mg-U/g-adsorbents) and capacity loss per use with 10 uses of H-ABP fiber in simulated seawater systems A & B

<b>Cycles</b>	1st	2nd	3rd	4th	5th	6 <sup>th</sup>	7th	8th	9th	10th	<b>Total</b>
<b>Simulated seawater system A</b>	290	298	299	300	302	278	251	234	201	187	<b>2640</b>
1		+2.8%	+3.1%	+3.4%	+4.1%	-4.1%	-13.4%	-19.3%	-30.7%	-35.5%	
<b>Simulated seawater system B</b>	5.73	5.78	5.86	6.13	6.68	8.66	6.23	5.10	4.93	4.14	<b>59.24</b>
1		+0.9%	+2.3%	+7.0%	+16.6%	+51.1%	+8.7%	-11.0%	-14.0%	-27.7%	
<b>Economic cost standard of adsorbents for recycling</b>	6.00	5.82	5.64	5.46	5.28	5.10	4.92	4.74	4.56	4.38	<b>51.90</b>
1		-3.0%	-6.0%	-9.0%	-12.0%	-15.0%	-18.0%	-21.0%	-24.0%	-27.0%	